Voluntary Respiration Control: Signature Analysis by EEG

Yue Wang, Yan Zhang, Yaoxi Zhang, Zongyu Wang, Weidong Guo, Yuru Zhang, *Senior Member, IEEE*, Yuhui Wang, Qinggang Ge, and Dangxiao Wang, *Senior Member, IEEE*

***Abstract*— The perception of voluntary respiratory consciousness is quite important in some situations, such as respiratory assistance and respiratory rehabilitation training, and the key signatures about voluntary respiration control may lie in the neural signals from brain manifested as electroencephalography (EEG). The present work aims to explore whether there exists correlation between voluntary respiration and scalp EEG. Evoke voluntary respiration of different intensities, while collecting EEG and respiration signal synchronously. Data from 11 participants were analyzed. Spectrum characteristics at low-frequency band were studied. Computation of EEG-respiration phase lock value (PLV) and EEG sample entropy were conducted as well. When breathing voluntarily, the 0-2 Hz band EEG power is significantly enhanced in frontal and right-parietal area. The distance between main peaks belonging to the two signals in 0-2 Hz spectrum graph tends to get smaller, while EEG-respiration PLV increases in frontal area. Besides, the sample entropy of EEG shows a trend of decreasing during voluntary respiration in both areas. There's a strong correlation between voluntary respiration and scalp EEG. Significance: The discoveries will provide guidelines for developing a voluntary respiratory consciousness identifying method and make it possible to monitor people's intention of respiration by noninvasive BCI.**

***Index Terms*— Respiration, EEG, PLV, sample entropy.**

Manuscript received 29 May 2023; revised 5 September 2023; accepted 2 October 2023. Date of publication 13 November 2023; date of current version 30 November 2023. This work was supported by the National Natural Science Foundation of China under Grant 82172553. *(Corresponding authors: Dangxiao Wang; Qinggang Ge.)*

This work involved human subjects or animals in its research. Approval of all ethical and experimental procedures and protocols was granted by the Peking University Third Hospital Medical Science Research Ethics Committee.

Yue Wang and Yuhui Wang are with the School of Mechanical Engineering and Automation, Beihang University, Beijing 100191, China.

Yan Zhang, Yaoxi Zhang, Weidong Guo, and Yuru Zhang are with the State Key Laboratory of Virtual Reality Technology and Systems, Beihang University, Beijing 100191, China.

Zongyu Wang and Qinggang Ge are with Peking University Third Hospital, Beijing 100191, China (e-mail: qingganggelin@126.com).

Dangxiao Wang is with the State Key Laboratory of Virtual Reality Technology and Systems and the Beijing Advanced Innovation Center for Biomedical Engineering, Beijing 102488, China, and also with Peng Cheng Laboratory, Shenzhen 518066, China (e-mail: hapticwang@buaa.edu.cn).

Digital Object Identifier 10.1109/TNSRE.2023.3332458

I. Introduction

RESPIRATION is the most basic and vital physiological process for maintaining human life, and the perception of respiratory consciousness is noteworthy in some situations. In our previous research, we developed a device to assist with coughing [1]. Although it can effectively facilitate phlegm clearance for bedridden patients, it requires manual initiation and cannot start automatically when the patients have phlegm, which undoubtedly adds to the caregiving time and manpower costs. Therefore, we propose a question: Can we find a method to monitor people's intention to cough? As coughing involves a rapid expiratory action, we elevated this question to a broader level: How can we identify people's consciousness of voluntary respiration control?

For those who participate in respiratory reinforcing or rehabilitation training, the aforementioned question also holds great significance of study. When people actively engage in the training, their respiratory function can be effectively enhanced [2], [3], [4], [5]. However, the repetitive exercise movement is often monotonous and can lead to boredom and fatigue, which can reduce people's focus and results in ineffective training, severely impacting the training efficiency. When people loss focus on the exercise, the consciousness of voluntary respiration control is lost as well. Thus, if this consciousness can be detected, people are able to be reminded when they are inattentive, by which achieving better reinforcement or rehabilitation results.

People have reached a consensus in the current physiology textbooks that, respiration movement originates from the rhythmic relaxation and contraction of the respiratory muscles under the control of the nerve center [6]. Automatic respiration rhythm comes from medulla oblongata without relying on cerebral cortex, while voluntary respiration is derived from the excitation of cortical neurons (Fig. 1, left). Hence, it can be inferred from one's electroencephalogram (EEG) that whether he/she participates actively in respiratory training. Existing researches on respiration and EEG are not rare, but most focus on the effect of respiration-related tasks [7], [8], [9], [10], while few directly analyze the differences in EEG characteristics when people breathe in the two disparate ways mentioned above.

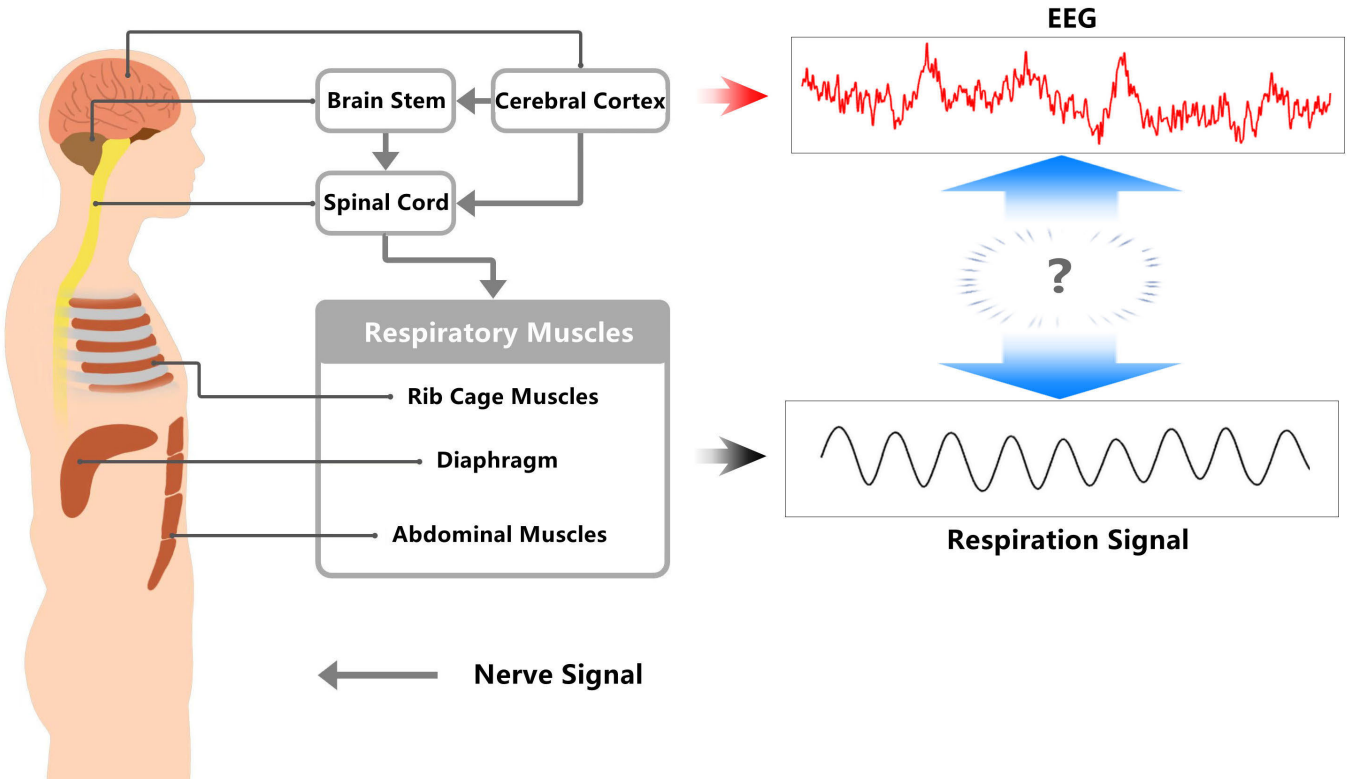

Fig. 1. Neural control of respiration (left) and the corresponding signal waveforms (right). The respiration-controlling nerve signals are generated by brain stem and cerebral cortex, and eventually act on respiratory muscles through spinal cord. When one's awake, cerebral cortex plays the role of the highest neural center. The respiration signal is periodical, while EEG is chaotic. Whether there are detectable connections between respiration and EEG is a question worth exploring.

Unlike periodic respiration signals, EEG is extremely chaotic and highly nonlinear in time domain (Fig. 1, right). Furthermore, EEG differs greatly in individuals. Thus, it's not easy to discover signatures of voluntary respiration in EEG. Nevertheless, a study of Herrero et al. [11] has shown some important conclusions. Based on intracranial electrodes, they found that the coherence between intracranial EEG (iEEG) and breath increases in some brain areas when people put attention to breathing. Their discoveries provide evidence for the existence of direct connection between EEG and voluntary respiration.

However, the acquisition of iEEG requires dangerous electrode implantation craniotomy, which is unacceptable for most patients with RD. Therefore, we propose a question: can we identify some respiration-related signatures from scalp EEG as the noninvasive brain computer interface (BCI) technology increasingly matures today? Compared to iEEG, scalp EEG can be conveniently collected by a wearable device without any surgeries. The difficulties lie in the facts that, scalp EEG is susceptible to interference from external environment and human body activities, and has lower spatial resolution and signal-noise ratio because the scalp hinders the signal transmission between the cerebral cortex and electrodes.

In the present work, we overcome the aforementioned difficulties and extract voluntary respiration-related signatures from scalp EEG for the first time, which suggests that the information about voluntary respiration control can be conveniently captured by utilizing non-invasive BCI. By analyzing several quickly computable time-domain, frequency-domain, and correlation signatures, EEG under voluntary respiration can be distinguished from that under automatic respiration in a very convenient way. Phase locking value (PLV) was generally only used for connectivity analysis of brain areas in previous studies, and we first applied it to analyze EEG's correlation with respiration. The results show that voluntary respiration can have significant effect on scalp EEG in some particular areas. Based on these new discoveries, there may be a high feasibility to develop a method to identify people's consciousness of voluntary respiration control by noninvasive-acquired neural signals.

II. Method

A. Evocation of Automatic and Voluntary Respiration

As mentioned above, human respiration can be divided into automatic and voluntary patterns, according to physiology theories. The word "automatic" means one is still able to breathe without consciousness, while "voluntary" means breathing actively. Actually, automatic respiration accounts for the majority of entire life, especially night time for sleeping. When people need to phonate, eat, drink, and so on, cerebral cortex will take over control from brain stem, and adjust respiration rhythm into a state they think. For example, people would hold their breath to avoid choking at the time they swallow a jelly, also breathe deeper and faster when they feel running out of oxygen.

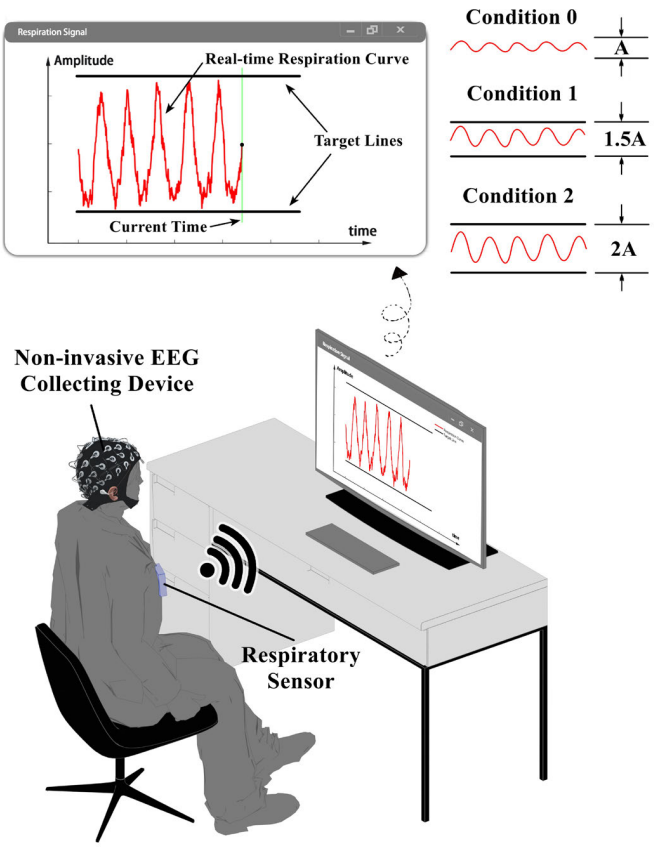

Fig. 2. The scene of the experiment in different conditions. In condition 0, signals won't be shown on the screen in order to avoid the participants receiving any hint about respiration. Top is a magnifying screen view of the task in condition 1 and 2. The red curve shows the real-time respiration wave monitored by sensors. In these two conditions, all participants are required to maintain a consist respiratory rate and breathe smoothly, finishing the task that training themselves breathing harder to raise the peaks and lower the troughs in order to get nearer to two target lines. Level of the task changes with the distance between the lines, larger distance corresponds to higher level. For example, the distance is set 1.5 times the amplitude of calm respiration (denoted by variable A like it shows in the top right-hand corner) in condition 1, and twice in condition 2.

In our experiment, we set 3 conditions to evoke the participants into different respiration patterns, condition 0 corresponds to automatic respiration while condition 1 and 2 to the other pattern.

Condition 0 (calm condition) is set at the beginning. When it starts, the participants will be told to keep relaxed in a chair but open their eyes up for minutes (the opening and closing states of eyes can obviously impact the alpha band of EEG signal, sees in Gilmore's research [13]), and focus on a simple picture which is displayed on the screen in front of them at the same time, so as to prevent them from concentrating on their respiration and breathe automatically. The maximum and minimum of respiration signal in this condition are determined in background and will be used to calculate the amplitude of automatic respiration.

Condition 1 and 2 are set right after condition 0. At this stage, the participants are required to finish a one-minute task by controlling their breath like it shows in Fig. 2. The real-time respiration signal will be shown on the screen as a moving curve, and they should breathe harder to make the curve reach the location of two horizontal lines. In this task, the participants are no doubt in the state of voluntary respiration because of forced breathing. There are two levels of difficulty, depending on the distance between target lines. The distance will be set 1.5 times the amplitude of automatic respiration in condition 1, and twice in condition 2, which means the expected amplitude respectively increases by 50% and 100% compared to condition 0. Each participant is allowed to try several times to get a better result before the formal experiment. The way to record respiration signal will be introduced in next section.

All participants will take a rest for over 10 minutes to get completely relaxed when they arrive. To further ensure the preciseness of condition 0, we make sure that none of them know the purpose of the experiment before tasks in condition 1 begins. Every level of task in condition 1 and 2 will repeat for three trials to eliminate some possible accidental data and make the result more universal and convincing. The room will be kept quiet to avoid them hearing noises which may causing interference on EEG.

B. Data Collection

The sampling system of our experiment consists of an EEG acquisition module, a respiration monitoring module, and supporting software on the computer.

Considering that the active brain areas of voluntary respiration are still quite unclear in existing researches, we use a wearable device with 59 electrodes (Fig. 3(A)) which can cover the whole scalp to record the potential changes near the brain at a 1,000 Hz sampling rate. By using both ears as reference electrodes, the collected signal can have better quality on account of the suppression of electrocardiography [14]. Through the accompanying receiver and router (Fig. 3(B)), the electrode cap is able to communicate wirelessly and accurately with computer in low time delay.

Generally, people use an airflow meter or barometer to monitor respiration, which requires a high level of airtightness. For those who in mechanical ventilation, the measurement of gas parameters can be easily done by sensors installed in the gas circuit of a ventilator, but it does not fit healthy people and a large quantity of patients who are not so seriously ill.

Inertial measurement unit (IMU) is a tiny sensor that has been widely used in the measurement of kinematic parameters like velocity, acceleration, and attitude angles. In addition to its small volume, IMU also has the advantage of acute sensitivity. When breathing, the thorax moves cyclically with the rhythm of respiration. In this work, we attach an IMU to the chest like it shows in Fig. 4(A), so that the respiration signals can be clearly expressed as the motion of chest and recorded in computer. Fig. 4(B) shows how the motion is measured, a_Z represents the measured acceleration of IMU in the Z-axis direction perpendicular to its upper surface, which is equal to the difference between the acceleration of chest undulation motion a and the component of gravity acceleration in that direction $-g\cdot\cos\theta$. In practice, the value of a is very small compared to the latter and can be ignored. In this research, the ratio of a_Z to g is actually recorded.

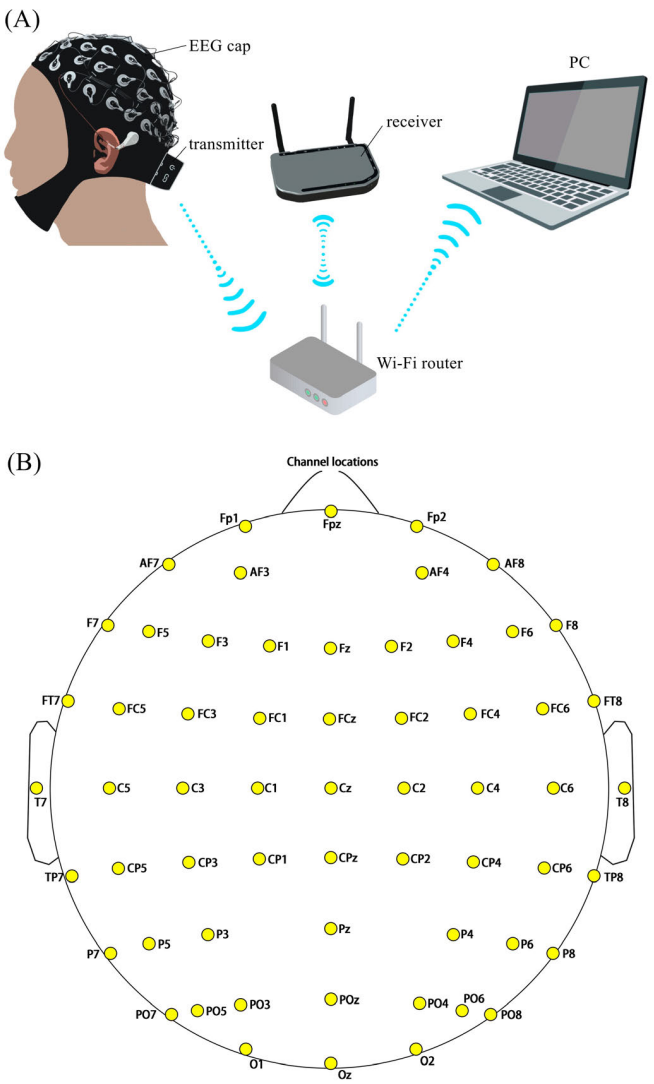

Fig. 3. Details of EEG collecting device. (A) The device to record EEG. Components include an wearable electrode cap, a receiver, and a Wi-Fi router. EEG is collected by the cap, then gathered and filtered by the receiver, and finally arrives at the computer, while the Wi-Fi router serves as a signal relay. To ensure good contact between electrodes and scalp, a kind of specially made conductive paste was added to each hole. (B) Allocation of EEG electrodes. Each electrode channel corresponds to a specific location on the scalp [15]. In this research, the channel CPz is only set for re-reference and calculated by CP1 and CP2, but its electrode doesn't really exist.

In fact, it's not the first use of IMU in respiration monitoring, quite a lot previous studies show that IMU can done the job as well as a sensing mask [16], [17], [18], [19]. The communication between IMU and computer is based on Modbus protocol [20]. The data collected in the latest 5 seconds will be stored in an array and keep updating on the screen, so that a real-time curve can be shown to the participants.

For the rigor of subsequent analysis, EEG and respiratory signals are collected synchronously in our experiment. Given that the sampling rate of IMU (100 Hz) is not the same as the EEG collector, a "start-to-end" strategy is adopted instead of recording at a constant interval. In this strategy, both sensors

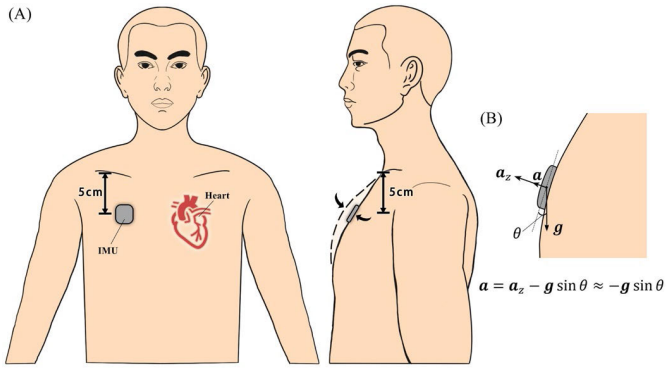

Fig. 4. (A) The installation position of IMU. The small sensor cube is sticked about 5cm below the right clavicle, a place with the largest chest undulation and weaker heartbeat noise in signal than the left side. (B) The measurement principle of IMU. The Z-axis acceleration a_z can be directly measured by the sensor, and has a mathematical correlation with the angle θ between the chest surface and the vertical direction. As people breathe, θ undergoes periodic changes.

are previously programed to start or end sampling at their respective frequencies when they receive a specific string. The special string message will be transmitted simultaneously through serial port at the exact time the experiment begins or finishes, so that the synchronization of data from different sensors is ensured. After recording, data from IMU will be interpolated to the same quantity as EEG for the convenience of matrix calculation.

To obtain better data quality, all participants are required to keep still with a fixed sitting posture and breathe stably without interfering behaviors such as blinking, eyes rolling, and coughing when the collection is going on [21] and [22].

C. Data Preprocessing

Preprocessing of data is very important before formal analysis, because of the noise and offset in original signals. The main interference in respiration signal is from the heartbeat. Whereas the power of heartbeat noise is much lower than the main signal, we use the method of moving average filter to deburr the data. A filtering window with the length of 150 is selected to do the convolution after several tests, which can get the best smoothing effect (Fig. 5). When the filtering is done, average value of the whole signal will be subtracted to remove any offset, so we can get the final detrended curve.

The preprocessing of EEG data is based on EEGLAB, a dedicated tool in MATLAB to do the calculation of EEG. A series of filtering operations are applied to original EEG dataset, which include a high-pass filtering at the frequency 0.1 Hz, a low-pass filtering at 40 Hz, and a band-stop filtering at the interval 49-51 Hz for further clearance of powerline interference. The assumed channel CPz is calculated and set as re-reference to improve signal-to-noise ratio [23]. Baseline correction runs as the next step to remove DC component of each channel.

Although we've set quite strict rules for participants to avoid physiological artifacts in EEG, ocular interference is still difficult to refrain. Therefore, we first manually removed the intervals that contained eye-blinking artifacts in data from all participants. Independent component analysis (ICA) has

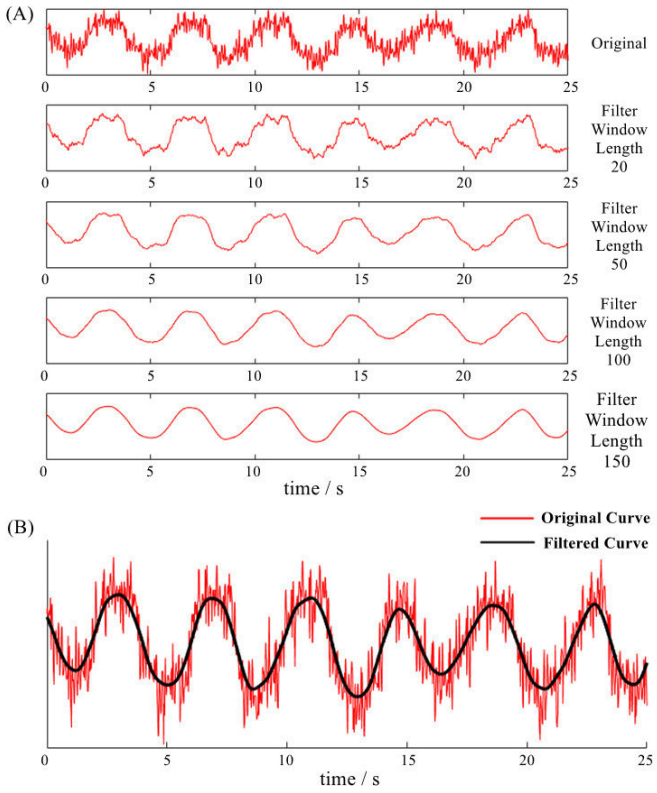

Fig. 5. IMU Data preprocessing, a section of data with a length of 25s is used as an example. (A) Comparison of different filter window lengths on respiration data. The length of 150 can best deburr the curve. (B) Comparison before and after filtering. The smooth filtered curve is easy to distinguish the amplitudes of different conditions.

been proved to be an effective algorithm to correct artifacts especially caused by eyes [24], [25]. The theory of ICA believes that signal and artifact are independent of each other, which means the original data can be decomposed into parts with different characteristics [26]. With the help of existing researches and pre-experiment, electrooculogram (EOG) artifact can be easily detected in the graphical interface of EEGLAB and removed.

D. Spectrum Calculation

Welch method is used in spectrum analysis. Compared with using Fourier transform directly, Welch method can effectively reduce the variance of spectrum [27].

Before the calculation, Standardize each segment of the signal as the following method

$$\boldsymbol{x}_{\text{std}} = \frac{\boldsymbol{x} - \bar{\boldsymbol{x}}}{\sigma_x} \tag{1}$$

where $\boldsymbol{x}_{\text{std}}$ is the standardized signal vector, $\boldsymbol{x}$ is the original signal vector, $\bar{\boldsymbol{x}}$ represents the baseline of $\boldsymbol{x}$ calculated by average, and $\sigma_{\boldsymbol{x}}$ is the standard deviation of $\boldsymbol{x}$.

In periodogram method, the power spectral density of signal is calculated by

$$P(f) = \frac{1}{NF_s}\left|\sum_{n=1}^{N} x(n) w(n) e^{-2\pi i f n / F_s}\right|^2 \tag{2}$$

where N is the number of points in vector x_{std}, F_s is the sampling frequency, i is the imaginary unit, and w is the window function used to assign different weights to points (all weights are set to 1 in general, which is called a rectangular window).

As for Welch method, the original signal is divided into several overlapping data segments of length M, which is denoted by

$$\boldsymbol{x}_j = \left(x_j(1), x_j(2), \ldots, x_j(M)\right)^T \tag{3}$$

Then, calculate the spectrum of each $\boldsymbol{x}_j$ by periodogram method as $P_j(f)$, and the final spectrum is estimated as follow

$$P_W(f) = \frac{1}{k}\sum_{j=1}^{k} P_j(f) \tag{4}$$

where k is the number of data segments.

In the analysis of subsequent chapters, we select a rectangular window with the length of 2,000 and a 50% overlap rate.

E. Phase Synchronization Analysis

Theoretically, voluntary respiration is a behavior under the control of brain, and the transmission of neural signals takes time. Thus, there might be a fixed time delay between the two signals, which can be reflected by the phase difference.

PLV (phase locking value) is one of the common indicators for evaluating phase synchronization [28], which has been widely used for connectivity analysis. PLV between signal vectors $\boldsymbol{x}$ and $\boldsymbol{y}$ is computed as

$$\text{PLV}_{\boldsymbol{xy}} = \left|\frac{1}{N}\sum_{n=1}^{N} e^{i\Delta\varphi(t_n)}\right| \tag{5}$$

$$\Delta\varphi(t_n) = \varphi_{\boldsymbol{x}}(t_n) - \varphi_{\boldsymbol{y}}(t_n) \tag{6}$$

$$\varphi_{\boldsymbol{x}}(t_n) = \tan^{-1}\frac{\boldsymbol{x}_{\text{H}}(t_n)}{\boldsymbol{x}(t_n)} \tag{7}$$

$$\varphi_{\boldsymbol{y}}(t_n) = \tan^{-1}\frac{\boldsymbol{y}_{\text{H}}(t_n)}{\boldsymbol{y}(t_n)} \tag{8}$$

where N is the number of sampling points, i is the imaginary unit, $\Delta\varphi(t_n)$ is the phase difference between the analytic signals of $\boldsymbol{x}$ and $\boldsymbol{y}$ at time t_n, $\Delta\varphi_x(t_n)$ and $\Delta\varphi_y(t_n)$ are the instantaneous phase of $\boldsymbol{x}$ and $\boldsymbol{y}$ which is calculated by (8) and (9). Moreover, $\boldsymbol{x}_{\text{H}}$ and $\boldsymbol{y}_{\text{H}}$ are the Hilbert transform of $\boldsymbol{x}$ and $\boldsymbol{y}$.

If PLV is equal to 1, then the analyzed signal vector $\boldsymbol{x}$ and $\boldsymbol{y}$ has a constant phase difference during the time period t_1 to t_N. On the contrary, if PLV is equal to 0, it means there's no phase synchronization between the two signals. In most cases, PLV is between 0 and 1.

F. Nonlinear Features

The neural activity of the human brain reflected in EEG is quite complex and unsteady. Therefore, methods related to nonlinear dynamic theory are beneficial to find some characteristics which is helpful for explaining the neurophysiological process of brain. Various nonlinear dynamic algorithms have been applied to EEG analysis so far, which demonstrate

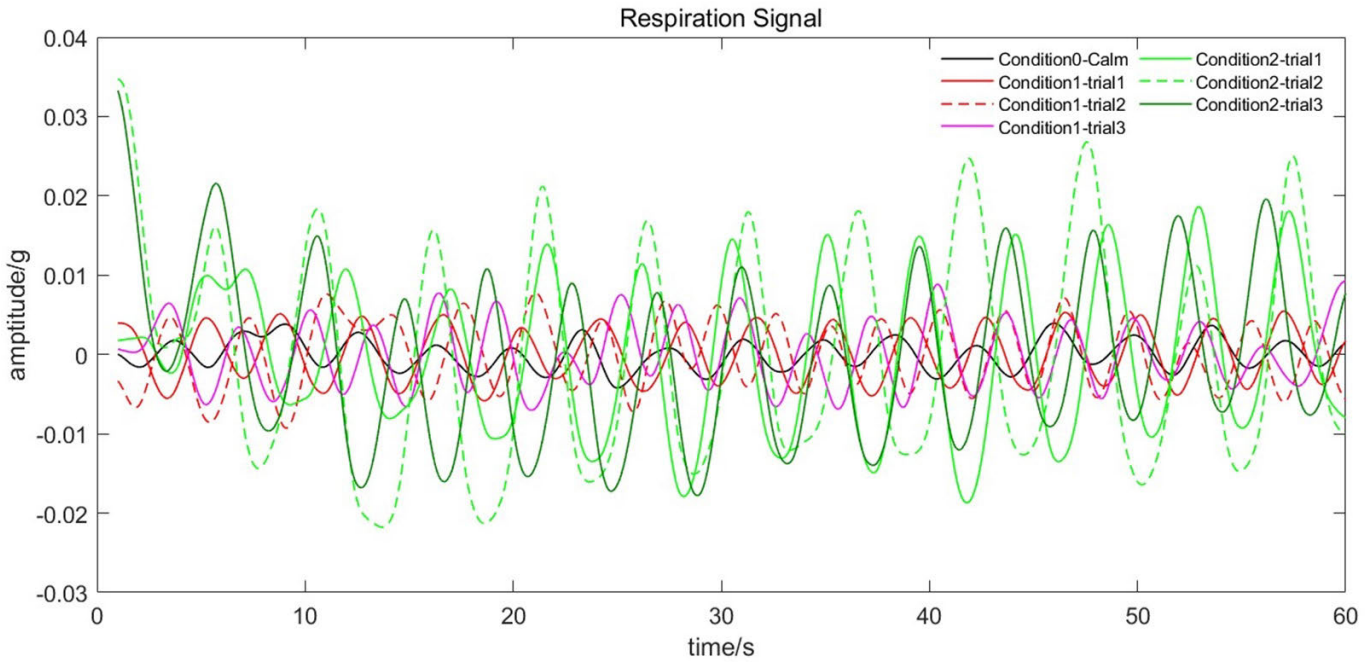

Fig. 6. The recorded respiration data from a participant after processing of filtering and detrending. Curves with different colors represent the results of different trials.

the nonlinear characteristics of EEG signals from different levels. Among these EEG analysis methods, the application of complexity and entropy is particularly widespread.

Here, we use sample entropy (SE) as an indicator to characterize the nonlinear complexity of EEG. We only list a few key steps of calculation, and the complete steps can be found in Richman et al.'s study [12].

First of all, we use the same method as formula (1) to get the standardized signal vector $\boldsymbol{x}$. Create $(N-m+1)$ vectors $\boldsymbol{x}_i$ by

$$\begin{aligned} \boldsymbol{x}_i &= \{x(i), \ldots, x(i+m-1)\} \\ i &= 1, 2, \ldots, N-m+1 \end{aligned} \tag{9}$$

where N is the number of points in $\boldsymbol{x}$, and m is the embedding dimension which is often taken as 2.

Let C_i be the probability that the distance between vector $\boldsymbol{x}_i$ and $\boldsymbol{x}_j$ is less than r, computed as

$$C_i = \frac{1}{N-m+1} \sum_{j=1}^{N-m+1} \Theta\left(d_{ij} - r\right) \tag{10}$$

where Θ is the Heaviside function, and d_{ij} is calculated by

$$\begin{aligned} d_{ij} &= \max\left(|x(i+k) - x(j+k)|\right) \\ k &= 0, 1, \ldots, m \end{aligned} \tag{11}$$

Define two variables A and B in (12) and (13)

$$A = \frac{1}{N-m} \sum_{i=1}^{N-m} C_i \tag{12}$$

$$B = \frac{1}{N-m+1} \sum_{i=1}^{N-m+1} C_i \tag{13}$$

Then, the sample entropy of $\boldsymbol{x}$ can be described as

$$\mathrm{SE} = -\ln\frac{A}{B} \tag{14}$$

The higher the value of SE, the more chaotic the signal is. The parameters we choose in this work are $m = 2$ and $r = 0.2$.

G. Participants

In total, 18 participants (aged from 18∼28) were recruited. Among them, 5 participated in the pre-experiment which was planned to verify the feasibility and discover potential vulnerabilities in our plan, such as whether the sensors with different sampling rate could work together normally, and whether the sitting posture could affect the baseline of respiration signal. The rest 13 participants completed the formal experiment with the same requirements and standards. Each of them promised not having any neurological or brain diseases before the experiment started. Data from 2 participants showed obvious abnormal fluctuations, which was deemed not to be directly related to voluntary respiration. Later, it was proved to be caused by frequent blinking of the eyes. Thus, we had to abandon these two pieces of data and retain data from the other 11 participants for subsequent analysis. The informed consent was obtained from all participants.

III. Result and Discussion

A. View of Respiration Data

Fig. 6 shows the recorded respiration data from a participant. The black curve corresponds to automatic respiration, while the red and green curves correspond to the two conditions set in our experiment.

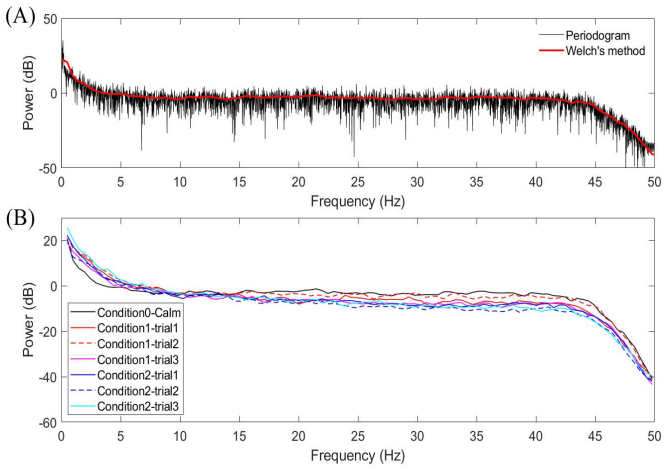

Fig. 7. (A) Comparison of spectra obtained by Welch method and periodogram method. (B) A graph with data collected in all conditions of channel F8 from a participant.

It can be seen that the amplitudes of different conditions are consistent with our expectations, which proves that we have successfully evoked voluntary respiration of different intensities. It can be also seen that, the respiration of participant in this figure is not stable at the beginning of condition 2 because the baseline is above the 0 position. For the other participants, this problem is not uncommon. Therefore, we will remove the 0-10s segment of data and retain the 10-60s segment in the subsequent analysis.

B. EEG Spectrum Analysis

Fig. 7(A) shows the comparison of two spectrum estimation method with a same EEG signal vector. Compared to periodogram method, Welch method can reflect the trend of signal power variation with frequency more clearly and effectively reduce the variance.

For each channel of a single participant, we plot the obtained EEG spectra under different conditions on the same graph, as shown in Fig. 7(B). Through preliminary observation of spectra of every channel from all participants, we found a common phenomenon that in a low-frequency band, the curve of condition 0 is below the others of condition 1 and 2, which means the signal power of some channels in condition 1 and 2 is higher than that in calm condition. Therefore, we assume that low-frequency EEG in some specific brain areas will be enhanced during voluntary respiration.

Generally, EEG signals can be divided into five components with different frequency bands: δ waves (0-4 Hz), θ waves (4-8 Hz), α waves (8-13 Hz), β waves (13-20 Hz), γ waves (>30 Hz). Among these, the band of δ waves which fall within the low-frequency range is of particular interest to us.

To validate our assumption, we computed the percentage of δ wave energy in the signals from various electrodes for all participants. Based on these calculations, a group of topographic maps are able to be generated, as it illustrates in Fig. 8(A). The results for conditions 1 and 2 are averages across the three trials. From the topographic maps in Fig. 8(A), it can be observed that the distribution of δ-EEG power percentage on the scalp among participants varies under the three conditions. However, this variation is not consistent. For instance, for participant 10, there is a noticeable δ-EEG power increase in the frontal region under Conditions 1 and 2, but this pattern does not hold true for participant 5.

Theoretically, voluntary respiration involves the brain's active control of movements of respiratory muscles, characterized by low-frequency rhythms. Given that the motor cortex is situated in the frontal lobe, low-frequency EEG signals in the frontal area during voluntary respiration should exhibit a macroscopic unified variation. We hypothesized that these variations might be present in signals of even lower frequency, and the 0-4 Hz δ-wave frequency band is possibly not sufficiently narrow for our analysis.

Consequently, we narrow down the frequency range to half (0-2 Hz) and generate another group of topographic maps, as shown in Fig. 8(B). From this subfigure, we notice that the differences between conditions are more pronounced in the 0-2 Hz frequency range. Although the distribution and range of value still differ a lot between participants, the changes from calm condition to condition 1 and 2 in some areas are consistent. Compared to calm condition, the power of signal from channels in frontal area (Fp1-Fp2, Fpz, AF3-AF4, AF7-AF8, F1-F8, Fz) and right-parietal area (CP4, CP6, TP8, P4, P6, P8, PO4, PO6, PO8) is higher in condition 1 and 2. This provides support for our hypothesis.

0-2 Hz band power from areas mentioned above is calculated by average to further compare the statistical differences. Considering rigorousness, in order to eliminate eye movement interference which usually has great influence on Fp and AF channels, only the rest 9 channels (F1-F8, Fz) in frontal area were analyzed. Fig. 9 is plotted as a result, and it's significant that condition 1 and 2 have generated stronger low-frequency EEG components than calm condition because p_1 and p_2 are higher than p for the vast majority of participants (p, p_1 and p_2 respectively denote 0-2 Hz power in different conditions). The above results are sufficient to indicate that, within the selected 0-2Hz frequency range, there exist signatures related to voluntary respiration in scalp EEG.

C. Joint Analysis of EEG and Respiration Signal

Another question worth figuring out is that whether there is a certain connection between EEG and respiration signals. In this section, a series of joint analyses are conducted.

We extracted the 0-2Hz EEG by a digital filter, and performed spectral analysis by Welch method in conjunction with respiratory signals. We observe that both types of signals exhibited spectral peaks within the 0-0.4 Hz frequency range, and each displays a prominent main peak. We use Δf to describe the distance between the two peaks, and record the results in Table I (the values from different trials in the same condition are averaged across the selected electrodes). In order to provide a clearer presentation of the calculation method for Δf and the peak distribution, we select 2 representative set of data from participants 1 and 9 (due to space limitations, we only show the two datasets), plotting the normalized time-domain signals and spectrum as shown in Fig. 10.

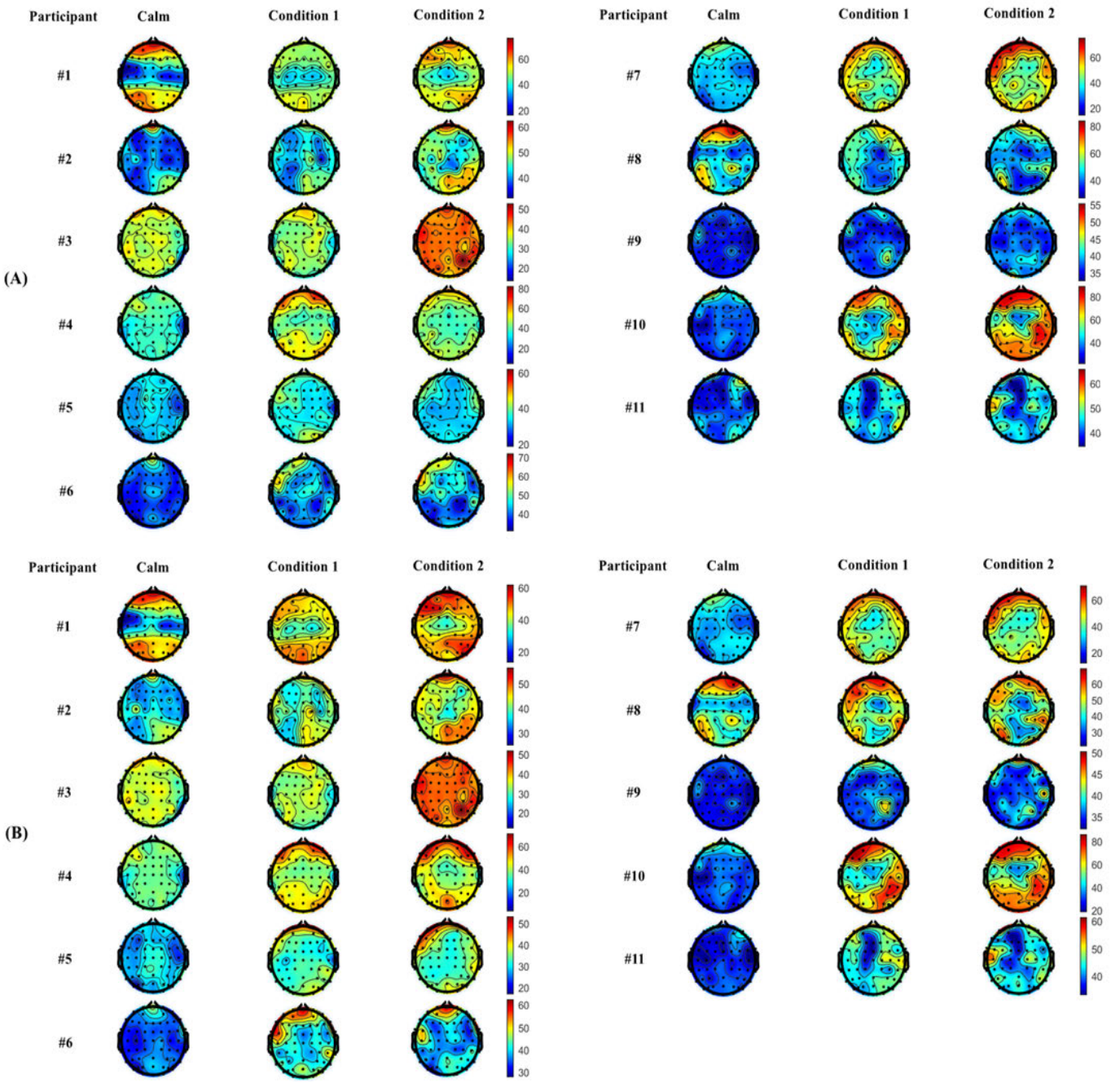

Fig. 8. EEG power percentage topographic maps in different conditions from all participants. (A) δ-EEG. (B) [0-2Hz]-EEG. Data from the same participant shares a same color bar. The allocation of electrodes is shown in Fig. 3(B).

From the table, it can be observed that in frontal area, Δf of data in condition 1 and 2 are significantly lower than that in condition 0. Furthermore, for the majority of participants, Δf of data in condition 2 are the smallest. This indicates that with increasing intensity of voluntary respiration, the main frequency in 0-2 Hz frontal EEG tends to align more closely with the breathing frequency. However, in right-parietal area, this conclusion does not hold true for every participant.

Additionally, it's worth noting that participants 8, 9, and 11 exhibit very close-to-zero Δf values in frontal area during voluntary respiration, which means their spectral main peaks nearly overlap like it shows in the right plot of Fig. 10. Upon inspecting the time-domain signals, a strong correlation between them becomes apparent. However, for the rest 8 participants including participant 1, the distance of peaks only narrows instead of completely overlapping. Whether these inter-participant differences arise from inherent individual variations or are a result of insufficiently stringent experimental conditions requires further in-depth investigation.

Power spectral density only reflects the amplitude of various frequency components, but it does not incorporate phase information from the spectrum. Hence, we also computed the average PLV across the selected electrodes in the aforementioned areas, and the results are presented in Fig. 11. It can

TABLE I
A SUMMARY OF THE MAIN PEAK DISTANCE

Participant No.	Frontal Area			Right-parietal Area		
	Calm	Condition 1	Condition 2	Calm	Condition 1	Condition 2
1	0.239	0.148	0.060	0.252	0.148	0.024
2	0.224	0.129	0.084	0.107	0.111	0.081
3	0.193	0.099	0.093	0.182	0.093	0.071
4	0.163	0.123	0.053	0.144	0.132	0.030
5	0.182	0.136	0.147	0.155	0.239	0.136
6	0.124	0.098	0.084	0.094	0.093	0.099
7	0.187	0.068	0.041	0.103	0.091	0.097
8	0.110	0.007	0.006	0.152	0.035	0.011
9	0.170	0.008	0.009	0.148	0.015	0.017
10	0.155	0.066	0.072	0.132	0.113	0.075
11	0.136	0.015	0.015	0.142	0.029	0.024

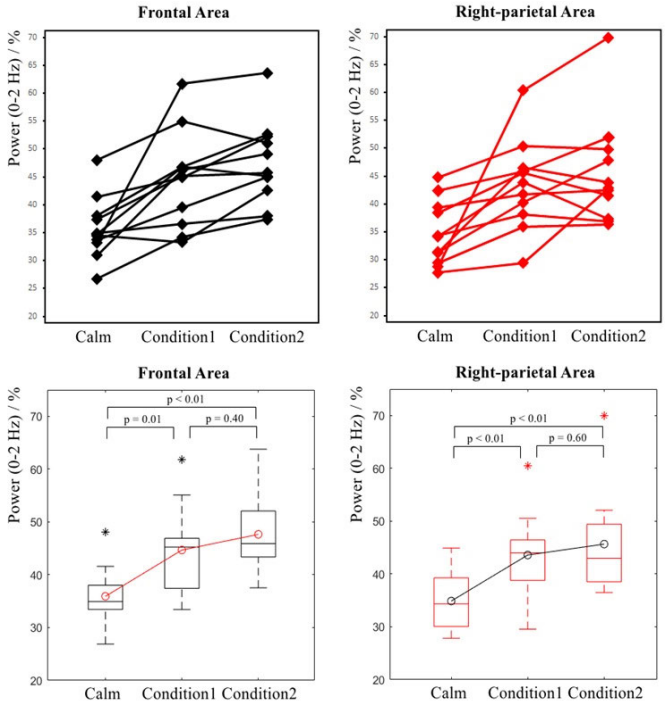

Fig. 9. A statistic of 0-2 Hz band power (described as variable P) in different conditions and brain areas. The broken line plots (top) show the changes of P in different conditions, each broken line represents data from one participant. The boxplots (bottom) further display the differences between conditions, the marker "$*$" represents outliers, and p denotes the significance level (by t-test). Moreover, the trend of average value is displayed as well.

be apparently seen that PLV between EEG (<2 Hz) and respiration signal shows an increasing trend and gets closer to 1, which means the phase synchronization is more obvious when the participants breath harder.

We propose an explanation to the phenomenon. During voluntary respiration, the action of the respiratory muscles is the result of the nerve signals from the cerebral cortex. These signals (we temporarily call them direct breathing commands, DBC) are generated by a group of cortical neurons in some specific brain areas, with a waveform similar to the respiration signal but with an advance in phase (as a result of the time delay in neural transmission). Due to the blocking effect of the scalp and skull, as well as the interference between signals from different brain areas, the phase advance in scalp EEG is not so significant, resulting in PLV of less than 1. As the intensity of respiration grows, the weight of DBC in scalp EEG increases likewise, which leads to the rise of PLV.

D. Nonlinear Analysis

Here's an explanation of the relevant variables before presenting the results. Let variable SE_0, SE_1, SE_2 respectively represent the sample entropy of EEG in condition calm, 1 and 2, and we use dSE_1 and dSE_2 to describe the percent rate of change from SE_0 to SE_1 and SE_1, i.e.

$$dSE_1 = (SE_1 - SE_0) \cdot 100\% \tag{15}$$

$$dSE_2 = (SE_2 - SE_0) \cdot 100\% \tag{16}$$

If dSE_i ($i = 1$ or 2) is a negative value, it indicates that EEG in condition i has a lower degree of chaos than calm condition. Fig. 12 shows the value of dSE_1 and dSE_2 in different scalp areas. By contrast with directly displaying the value of sample entropy, we can get a better comparison result in this way. As it can be seen, most data points are below the zero line, and the distribution of dSE_2 value is lower than dSE_1, from which we can deduce that EEG in frontal and right-parietal area tends to be more orderly when breathing voluntarily.

We can explain this phenomenon from a physiological perspective. Considering that voluntary respiration is controlled by the cerebral cortex, the brain will continuously send nerve

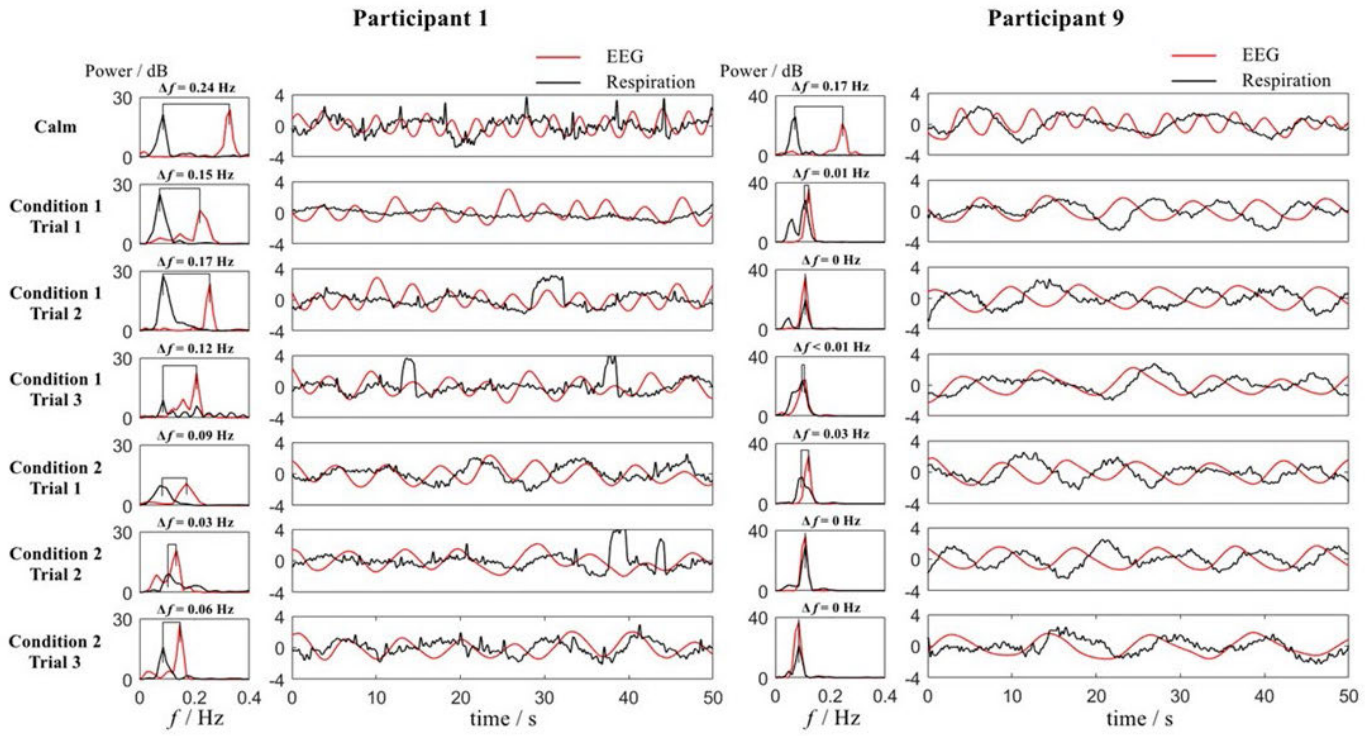

Fig. 10. The spectrum and time domain signal graph from data of two participants who respectively represents one typical peak distribution. For each participant, the right column presents EEG (<2 Hz) and respiratory signals of all experiment trials, while the left column shows the spectrum of 0-2 Hz. Range of 0.4-2 Hz are not displayed for a very low proportion of power by contrast with 0-0.4 Hz. The time domain EEG signals are from channel Fz, which is the center of frontal area. The positions of the main peak of the two signals in the spectrum are marked out, and Δf denotes the distance between the two peaks.

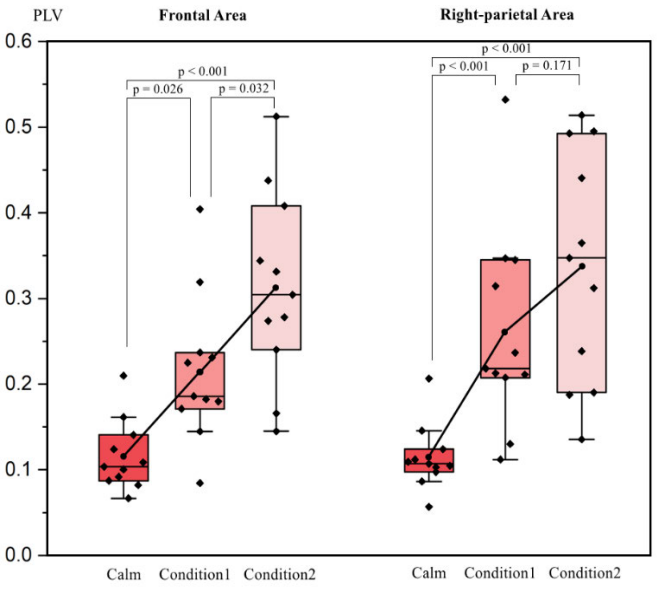

Fig. 11. A statistic of EEG (<2 Hz)-respiration PLV in different conditions and brain areas. Data from all participants are marked out in the boxplot, and p denotes the significance level (by t-test). Besides, the trend of average value is displayed by a black broken line as well.

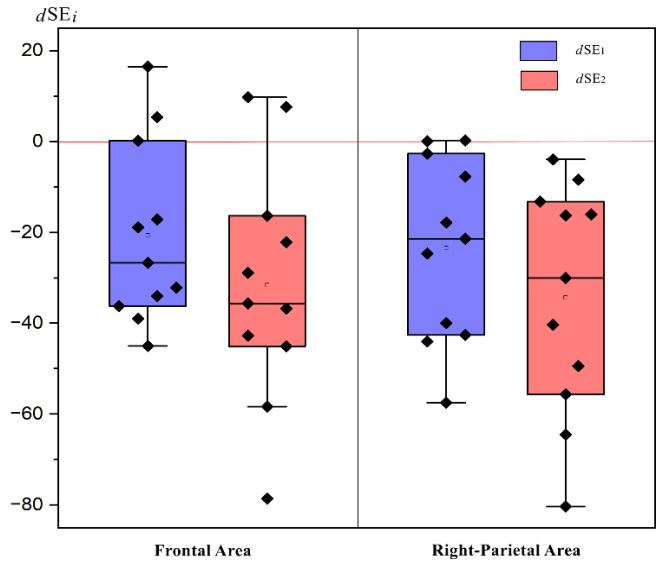

Fig. 12. The boxplot of dSE_i in frontal and right-parietal area. The definition of dSE_i sees in formula (15) and (16). A red horizontal zero line is also plotted for comparison.

signals to the respiratory muscles as hard breathing goes on. Although EEG itself is highly chaotic, respiration is a highly ordered activity, so as the respiratory-controlling signal components. When people put more strength on breathing, these components will also be enhanced. Hence, the chaos level of EEG has been reduced overall.

IV. Conclusion

We have analyzed data from 11 participants and calculated multiple signal characteristics to figure out whether there's a correlation between voluntary respiration and scalp EEG. The results manifest that this connection not only exists, but is also significant. From the conducted analysis, the specific impact of voluntary respiration on EEG includes the following aspects. In frequency domain, when people breathe

harder, the low-frequency EEG components within 2 Hz turn more active in frontal and right-parietal area, and the prominent main peak in the band of 0-2 Hz gets more closer to the frequency of respiration signal in frontal area. In time domain, there's a positive correlation between respiration intensity and EEG (<2 Hz)-respiration PLV. From the perspective of nonlinear dynamics, breathing voluntarily can decrease the sample entropy value of EEG, which means a more orderly state. The significance of this work lies in its demonstration of the potential to utilize a convenient noninvasive BCI for identifying respiratory consciousness. This could meet applications in various fields including respiratory assistance, respiration monitoring, and respiration signal feedback. Apparently, conclusions drawn at present do remain space for refinement, and cannot yet explain inter-individual differences, we believe that more rigorous experiments based on various populations in the future will address these gaps.

REFERENCES

[1] Y. Zhang et al., "Soft exoskeleton mimics human cough for assisting the expectoration capability of SCI patients," *IEEE Trans. Neural Syst. Rehabil. Eng.*, vol. 30, pp. 936–946, 2022.

[2] A. I. C. de Medeiros, H. K. B. Fuzari, C. Rattesa, D. C. Brandão, and P. É. de Melo Marinho, "Inspiratory muscle training improves respiratory muscle strength, functional capacity and quality of life in patients with chronic kidney disease: A systematic review," *J. Physiotherapy*, vol. 63, no. 2, pp. 76–83, Apr. 2017.

[3] M. Messaggi-Sartor et al., "Inspiratory and expiratory muscle training in subacute stroke: A randomized clinical trial," *Neurology*, vol. 85, no. 7, pp. 564–572, Aug. 2015.

[4] R. R. Britto, N. R. Rezende, K. C. Marinho, J. L. Torres, V. F. Parreira, and L. F. Teixeira-Salmela, "Inspiratory muscular training in chronic stroke survivors: A randomized controlled trial," *Arch. Phys. Med. Rehabil.*, vol. 92, no. 2, pp. 184–190, Feb. 2011.

[5] K. K. Menezes, L. R. Nascimento, L. Ada, J. C. Polese, P. R. Avelino, and L. F. Teixeira-Salmela, "Respiratory muscle training increases respiratory muscle strength and reduces respiratory complications after stroke: A systematic review," *J. Physiotherapy*, vol. 62, no. 3, pp. 138–144, Jul. 2016.

[6] T. Wang, "Respiration," in *Physiology*, 9th ed. Beijing, China: People's Med. Publishing House, 2018, pp. 147–176.

[7] M. Fumoto, I. Sato-Suzuki, Y. Seki, Y. Mohri, and H. Arita, "Appearance of high-frequency alpha band with disappearance of low-frequency alpha band in EEG is produced during voluntary abdominal breathing in an eyes-closed condition," *Neurosci. Res.*, vol. 50, no. 3, pp. 307–317, Nov. 2004.

[8] P. Bušek and D. Kemlink, "The influence of the respiratory cycle on the EEG," *Physiolog. Res.*, vol. 54, no. 3, pp. 327–333, 2005.

[9] A. von Leupoldt, P.-Y.-S. Chan, M. M. Bradley, P. J. Lang, and P. W. Davenport, "The impact of anxiety on the neural processing of respiratory sensations," *NeuroImage*, vol. 55, no. 1, pp. 247–252, Mar. 2011.

[10] M. S. Morelli et al., "Analysis of generic coupling between EEG activity and $P_{ET}CO_2$ in free breathing and breath-hold tasks using maximal information coefficient (MIC)," *Sci. Rep.*, vol. 8, no. 1, p. 4492, Mar. 2018.

[11] J. L. Herrero, S. Khuvis, E. Yeagle, M. Cerf, and A. D. Mehta, "Breathing above the brain stem: Volitional control and attentional modulation in humans," *J. Neurophysiol.*, vol. 119, no. 1, pp. 145–159, Jan. 2018.

[12] J. S. Richman and J. R. Moorman, "Physiological time-series analysis using approximate entropy and sample entropy," *Amer. J. Physiol.-Heart Circulatory Physiol.*, vol. 278, no. 6, pp. H2039–H2049, Jun. 2000.

[13] R. L. Gilmore, "American-electroencephalographic-society guidelines in electroencephalography, evoked-potentials, and polysomnography," *J. Clin. Neurophysiol.*, vol. 11, no. 1, pp. 1–147, 1994.

[14] M. Nakamura and H. Shibasaki, "Elimination of EKG artifacts from EEG records: A new method of non-cephalic referential EEG recording," *Electroencephalogr. Clin. Neurophysiol.*, vol. 66, no. 1, pp. 89–92, Jan. 1987.

[15] J. N. Acharya, A. Hani, J. Cheek, P. Thirumala, and T. N. Tsuchida, "American clinical neurophysiology society guideline 2: Guidelines for standard electrode position nomenclature," *J. Clin. Neurophysiol.*, vol. 33, no. 4, pp. 308–311, 2016.

[16] M. Rahman and B. I. Morshed, "Estimation of respiration rate using an inertial measurement unit placed on thorax-abdomen," in *Proc. IEEE Int. Conf. Electro Inf. Technol. (EIT)*, May 2021, pp. 1–5.

[17] R. K. Albright, B. J. Goska, T. M. Hagen, M. Y. Chi, G. Cauwenberghs, and P. Y. Chiang, "OLAM: A wearable, non-contact sensor for continuous heart-rate and activity monitoring," in *Proc. Annu. Int. Conf. IEEE Eng. Med. Biol. Soc.*, Aug. 2011, pp. 5625–5628.

[18] H. Jeong et al., "Differential cardiopulmonary monitoring system for artifact-canceled physiological tracking of athletes, workers, and COVID-19 patients," *Sci. Adv.*, vol. 7, no. 20, May 2021, Art. no. eabg3092.

[19] R. De Fazio, P. Visconti, E. Perrone, M. R. Greco, and R. Velazquez, "Development and testing of piezoresistive and inertial-based chest bands for breathing monitoring," in *Proc. 7th Int. Conf. Smart Sustain. Technol. (SpliTech)*, Jul. 2022, pp. 1–6.

[20] M. K. Islam, A. Rastegarnia, and Z. Yang, "Methods for artifact detection and removal from scalp EEG: A review," *Clinical Neurophysiol.*, vol. 46, nos. 4–5, pp. 287–305, Nov. 2016.

[21] S. Naskar, K. Basuli, and S. S. Sarma, "Serial port data communication using MODBUS protocol," *Ubiquity*, vol. 2008, p. 1, Jan. 2008.

[22] T. Jung et al., "Removing electroencephalographic artifacts by blind source separation," *Psychophysiology*, vol. 37, no. 2, pp. 163–178, Mar. 2000.

[23] A. Delorme and S. Makeig, "EEGLAB: An open source toolbox for analysis of single-trial EEG dynamics including independent component analysis," *J. Neurosci. Methods*, vol. 134, no. 1, pp. 9–21, Mar. 2004.

[24] S. Hoffmann and M. Falkenstein, "The correction of eye blink artefacts in the EEG: A comparison of two prominent methods," *PLoS ONE*, vol. 3, no. 8, p. e3004, Aug. 2008.

[25] M. Plöchl, J. P. Ossandón, and P. König, "Combining EEG and eye tracking: Identification, characterization, and correction of eye movement artifacts in electroencephalographic data," *Frontiers Hum. Neurosci.*, vol. 6, no. 278, pp. 1–23, 2012.

[26] Y. Zou, V. Nathan, and R. Jafari, "Automatic identification of artifact-related independent components for artifact removal in EEG recordings," *IEEE J. Biomed. Health Informat.*, vol. 20, no. 1, pp. 73–81, Jan. 2016.

[27] P. Welch, "The use of fast Fourier transform for the estimation of power spectra: A method based on time averaging over short, modified periodograms," *IEEE Trans. Audio Electroacoustics*, vol. AE-15, no. 2, pp. 70–73, Jun. 1967.

[28] J.-P. Lachaux, E. Rodriguez, J. Martinerie, and F. J. Varela, "Measuring phase synchrony in brain signals," *Hum. Brain Mapping*, vol. 8, no. 4, pp. 194–208, 1999.